Optical cross sections associated with deep-level impurities in semiconductors

J. Petit, G. Allan, and M. Lannoo
Laboratoire d'Etude des Surfaces et Interfaces, Institut Supérieur d'Electronique du Nord, 3 rue François Baës, 59046 Lille Cédex, France
(Received 19 November 1985)

Optical cross sections associated with deep-level impurities in semiconductors are calculated in the tight-binding approximation, using a Green's-function formalism. The calculations are performed by either neglecting or introducing the modifications undergone by the initial Bloch states in the vicinity of the impurity. Great differences are then observed that enable us to interpret some experimental data available on silicon.

I. INTRODUCTION

Optical cross sections (OCS) associated with transitions between bound states and band states of a semiconductor have often been calculated using perfect-crystal band structure and pure Bloch waves as band states.[1-4] Although some workers[5-7] have already shown, using simplified models, that a correct description of the band states could have great influence on the OCS calculated spectra, others[8] do not seem to agree with their conclusions. Our main interest here is to show the modifications undergone by the OCS, using either modified or unmodified band states.

With this aim, we develop a Green's-function formulation of the OCS in the tight-binding approximation. We treat the case of covalent and diamond structure semiconductors (the numerical calculations being applied to silicon). Our method enables us to introduce, in an easy manner, the modifications brought to band states by the defect potential using Dyson's equation. If one chooses a well-localized perturbation potential, one gets matrices of small size, numerical calculations then being considerably simplified. Our model is thoroughly presented in Sec. II. The results concerning silicon are presented in Sec. III. We put some emphasis on band states perturbation effects, but we also discuss the effects of the position of the energy level and the symmetry of the wave function associated with the bound state. Section IV is devoted to a comparison with experimental and other theoretical results available on silicon.

II. THE MODEL

The optical cross section associated with transitions between a localized state $|\Psi_L\rangle$ of energy E_L and the band states $|\Psi_{b,k}\rangle$ of energy $E_{b,k}$ is expressed as follows in the dipole approximation[9]

$$\sigma(h\nu)=\frac{\beta}{h\nu}\sum_{b,k}|\langle\Psi_L|p_z|\Psi_{b,k}\rangle|^2\delta(h\nu-|E_{b,k}-E_L|)$$

with

$$p_z=-i\hbar\frac{\partial}{\partial z}\quad\text{and}\quad\beta=\frac{4\pi^2e^2\hbar}{m^2cn}\left[\frac{E_{\text{eff}}}{E_0}\right]^2, \tag{1}$$

where $h\nu$ is the excitation energy associated to the radiation and z denotes the axis of the radiation polarization, n is the index of refraction, and E_{eff}/E_0 the so-called effective field ratio.[10]

Equation (1) may be rewritten into a well-suited form:

$$\sigma(h\nu)=\frac{\beta}{h\nu}\left\langle\Psi_L\left|p_z\sum_{b,k}|\Psi_{b,k}\rangle\langle\Psi_{b,k}|\times\delta(h\nu-|E_{b,k}-E_L|)p_z\right|\Psi_L\right\rangle . \tag{2}$$

Introducing the definition of the δ function,

$$\delta(h\nu-|E_{b,k}-E_L|)=\frac{1}{\pi}\lim_{\eta\to0^+}\frac{\eta}{(h\nu-|E_{b,k}-E_L|)^2+\eta^2}, \tag{3}$$

and the definition of the Green's operator,

$$G(E)=\lim_{\eta\to0^+}\sum_{b,k}\frac{|\Psi_{b,k}\rangle\langle\Psi_{b,k}|}{E-E_{b,k}+i\eta}, \tag{4}$$

we get

$$\sigma(h\nu)=-\frac{\beta}{\pi h\nu}\,\text{Im}\,|\langle\Psi_L|p_zG(E_L\pm h\nu)p_z|\Psi_L\rangle| \tag{5}$$

where Im denotes the imaginary part and the sign $+$ $(-)$ corresponds to a transition involving the conduction (valence) band. Green's functions (Green's operator matrix elements) are computed for the perfect crystal following the so-called Brillouin-zone integration method which is commonly used (see, for instance, Ref. 11).

Introducing a point defect (here, a substitutional impurity) adds a potential which can be supposed very localized, especially if the associated energy levels are found to be deep in the gap. The new resolvent (or Green's operator) G of the perturbed system is related to the resolvent G^0 of the perfect crystal by Dyson's equation:

$$G=G^0+G^0VG\ . \tag{6}$$

Only when the extension of the potential is very limited is this equation of easy use. Here we are going to consider a matrix V associated with the impurity potential having

terms different from zero on the perturbed site only. The impurity is supposed to be represented by four orbitals, just like a host crystal atom: s, p_x, p_y, and p_z. The matrix V is taken diagonal, that is, we consider a shift on the orbital energies of the impurity atom. The shift is identical for all types of orbitals. Its value will vary in order to simulate different kinds of impurities and energy-level positions in the gap.

This study concerns the diamond structure, which has two atoms per unit cell. We develop our calculations in a tight-binding scheme. We retain interactions between first and second neighbors only, and use the parameters of Van der Rest *et al.*[12] As regards the optical matrix elements, we include intra-atomic and nearest-neighbor interatomic contributions. These have been calculated representing atomic orbitals by Gaussians. Their values are listed, for silicon, in Table I.

III. THE RESULTS

A. The vacancy case

The vacancy case is represented in our model by a potential shift V tending to infinity as introduced first by Lannoo and Lenglart.[13] A calculation using the same model as we discussed above has already been performed by Bernholc and Pantelides.[11] Our results are of course in total agreement with theirs, provided we use the same parameters defined in Ref. 14. Introducing a new set of parameters,[12] giving better agreement with the results of local-density calculations,[15] leads to the following results:

(1) A bound state associated with the vacancy is found at 0.36 eV (all energies are referred to the top of the valence band). This state, of T_2 symmetry, is threefold degenerate.

(2) A resonant state of A_1 symmetry is found in the valence band at -0.68 eV (another one, also of A_1 symmetry, is found deeper in the valence band at -7.3 eV).

All these observations are consistent with other results on the vacancy in Silicon.[13–16]

TABLE I. Optical matrix elements expressed in an atomic basis set. A and B denote two first neighbor atoms. The axis x is chosen following the direction $A-B$. The values are expressed in atomic units. Other matrix elements are zero or are deduced from these by symmetry.

$\left\langle \phi_s(A) \left\| \frac{\partial}{\partial x} \right\| \phi_x(A) \right\rangle$	$=0.371$
$\left\langle \phi_s(A) \left\| \frac{\partial}{\partial x} \right\| \phi_s(B) \right\rangle$	$=0.155$
$\left\langle \phi_s(A) \left\| \frac{\partial}{\partial x} \right\| \phi_x(B) \right\rangle$	$=-0.165$
$\left\langle \phi_x(A) \left\| \frac{\partial}{\partial x} \right\| \phi_x(B) \right\rangle$	$=-0.081$
$\left\langle \phi_y(A) \left\| \frac{\partial}{\partial x} \right\| \phi_y(B) \right\rangle$	$=0.134$
$\left\langle \phi_x(A) \left\| \frac{\partial}{\partial y} \right\| \phi_y(B) \right\rangle$	$=0.134$
$\left\langle \phi_s(A) \left\| \frac{\partial}{\partial y} \right\| \phi_y(B) \right\rangle$	$=0.076$

B. Bound-state energy levels and wave functions

In the following, we consider the potential V as a variable so that we can obtain one or two bound states whose energy-level positions may vary from the lower to the upper edge of the band gap. We remember that the high localization chosen for the perturbation potential gives our results their best validity when the bound-state energy level is situated farther from the band edges, that is to say, when the associated wave-function extension is the most limited.

The bound-state energy levels E_L are given by the determinantal condition:

$$\det[I-G^0(E_L)V]=0\,, \tag{7}$$

giving here

$$1-VG^0_{ss}(E_L)=0 \tag{8}$$

or

$$1-VG^0_{pp}(E_L)=0\,, \tag{9}$$

where $G^0_{ss}(E)$ and $G^0_{pp}(E)$ are the diagonal Green's functions of the perfect crystal related to s and p orbitals, respectively. Equation (8) gives us the position of the A_1-type bound state while Eq. (9) is related to the T_2-type states (threefold degenerated). The curves $E_L=f(V)$ we obtain from these equations are plotted in Fig. 1.

The bound-state wave function is expanded in a localized atomic orbital basis (linear combination of atomic orbitals method) as

$$|\Psi_L\rangle=\sum_i a_i\,|\phi_i\rangle\,, \tag{10}$$

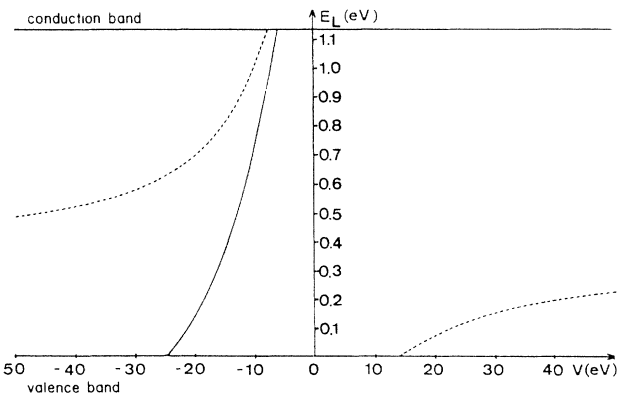

FIG. 1. Bound-states energy levels as functions of potential V for A_1 states (solid line) and T_2 states (dashed line).

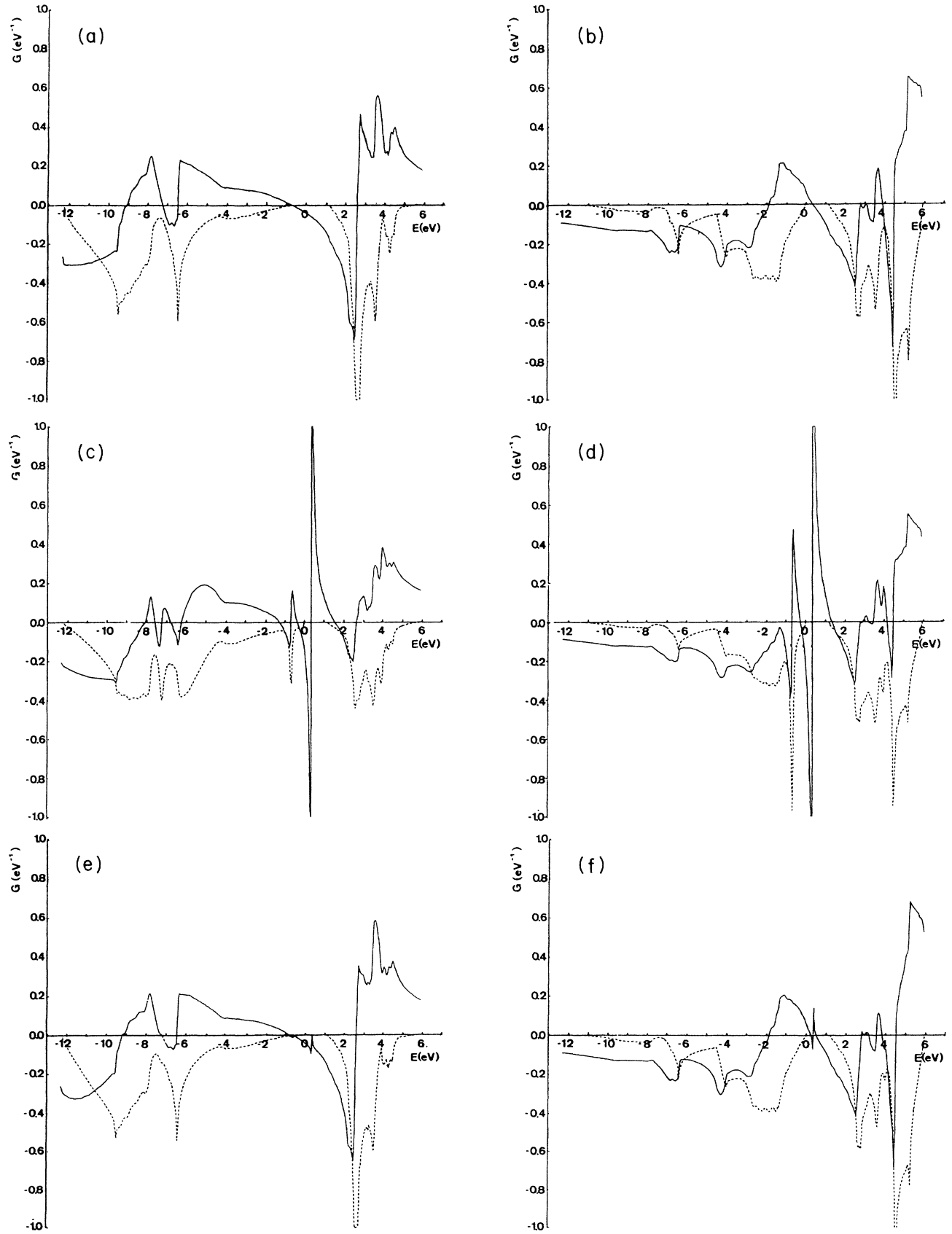

FIG. 2. Green's functions versus energy: ——, real part; — — —, imaginary part. (a) $G^0_{ss}(E)$ (perfect crystal); (b) $G^o_{pp}(E)$ (perfect crystal); (c) $G_{ss}(E)$ on a first neighbor of a vacancy site; (d) $G_{pp}(E)$ on a first neighbor of a vacancy site; (e) $G_{ss}(E)$ on a third neighbor of a vacancy site; (f) $G_{pp}(E)$ on a third neighbor of a vacancy site.

where i stands for an atom and orbital type index. $|\phi_i\rangle$ is the ith atomic orbital of the crystal.

The coefficients a_i are expressed in terms of Green's functions using the following equation:

$$(I-G^0V)|\Psi_L\rangle=0 \tag{11}$$

and calculated following a method described by Lannoo and Lenglart.[13]

As the number of computed Green's functions is necessarily limited, Eq. (10) should be truncated. A glance at the convergence properties of the Green's functions enables us to stop the expansion when we reach the third neighbors of the defect site. As an example, we represent in Figs. 2(a)–2(f) the diagonal s- and p-type Green's functions, respectively, for a host crystal atom, a first and a third neighbor atom of a vacancy. Rather good agreement is obtained between the curves corresponding to the third neighbor of the vacancy and that of the perfect crystal. Conclusions are the same when studying the extension of the localized state. We find that for a state whose energy level is deep enough, about 60% of the state is located on the first neighbors and we reach more than 80% when including first, second, and third neighbors for a T_2 symmetry bound state. These ratios are about 75% and 90%, respectively, when an A_1 symmetry bound state is considered as these states are shown to be more localized.[17] Moreover, we notice that when the bound-state energy level shifts towards band edges, localization tends to decrease, as expected from other theories (for instance, from effective-mass results.[2] Nevertheless, the decrease is very smooth, as the Green's functions also vary smoothly in the gap, so that the localization of a bound-state wave function is not strongly related to its energy-level depth in the gap (in contrast with effective-mass results).

C. Optical cross section

Here we are mainly interested in the effect on band states of the perturbation which is caused by the impurity potential. Equation (5) is there exploited introducing either G^0 (Green's operator of the perfect crystal), giving the OCS σ^0 corresponding to the unmodified band states, or G (Green's operator of the perturbed crystal), leading to the OCS σ, which takes into account band states scattering. We also discuss the results as a function of the energy-level depth and the symmetry type of the bound state. Transitions towards valence or conduction bands have been investigated. We first checked the convergence property of the calculation and found that good agreement was obtained when comparing the OCS curves, when second and third neighbors of the defect center are included, respectively.[17] This fast convergence may be explained by the convergence properties of the Green's functions we noticed before.

1. *Effect of the scattering of the band states*

For every figure of OCS studied here, we compare the curve when pure-crystal wave functions are used (σ^0, solid line) with the curve which takes into account scattering of the band states (σ, dashed line). Great modifications clearly occur. Firstly, peaks are sometimes observed on σ curves that can be attributed to resonant state effects, as will be seen later. Secondly, even in the absence of these peaks, the OCS are substantially modified when including band scattering effects, especially near thresholds for transitions, either towards valence or conduction bands. The general tendency in the regions near thresholds in the absence of resonant states is that σ is smaller than σ^0. This conclusion is different from that formulated by Jaros *et al.*[8] They discussed band scattering effects in terms of perturbations of the density of states of the crystal and concluded that only sharp resonances or antiresonances may alter the density of states. In fact it is clear, as the bound-state wave function is very localized, that only local densities of states near the defect center have to be considered (those densities that are mainly altered by the perturbation potential). We can easily prove this effect when treating the simplified case of a vacancy in a molecular model. The development is made in the Appendix. This effect is of great interest because, as we noticed earlier, transitions near thresholds are the most experimentally concerned. For higher photon energies, band-to-band transitions may occur and alter the shape of the OCS curve.

2. *Effect of the energy-level depth*

As a general remark, we may say that the closer the bound-state energy level is from the edge of the band involved in the transition, the greater the OCS. This is due to the $1/h\nu$ factor appearing in Eq. (1). Indeed, as the bound-state localization remains nearly independent of V, we may conclude that for a fixed value of $E_{b,k}$, the amplitude of σ^0 is essentially determined by the $1/(E_L-E_{b,k})=1/h\nu$ factor. The same conclusion may be applied to σ, provided that band states do not change significantly, that is to say when $|V|$ remains large.

First we consider transitions between the t_x bound state (of T_2 symmetry and transforming as x) associated with the vacancy and the valence band when the incident light is polarized along the [100] direction. The two peaks observed on the σ curve of Fig. 3 at $+1.04$ eV and $+7.66$ eV, respectively, can undoubtedly be related to the

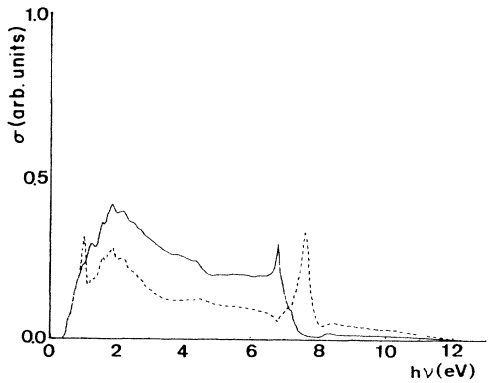

FIG. 3. OCS for transitions between the t_x bound state associated with the vacancy and the valence band when the light is polarized along the [100] axis. σ^0: solid line. σ: dashed line.

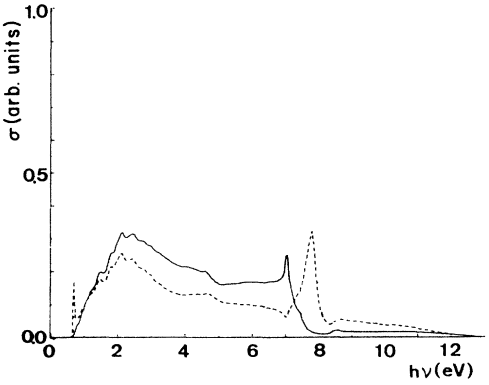

FIG. 4. OCS for transitions between the t_x bound state associated with $V=-30$ eV and the valence band when the light is polarized along the [100] axis. σ^0: solid line. σ: dashed line.

resonant states observed at the relevant energies in the local density of states around the vacancy [see imaginary parts of Green's functions of Fig. 2(c) and 2(d)].

The position of the resonant states is expected to shift when the potential V is varying. We show, in Figs. 4–6, transitions between the valence band and the t_x bound state for $V=-30$ eV, -10 eV, and $+20$ eV, respectively. When $V=-30$ eV, a glance at Fig. 1 enables us to guess that the A_1 resonant state is very close to the band edge. We verify this in Fig. 4. If V increases a lot, the A_1 state becomes a bound state (for $V=-10$ eV, for instance). Hence, no peak near threshold is observed in Fig. 5. On the other hand, when $V=+20$ eV, the A_1 resonant state is found deeper in the valence band (Fig. 6).

An equivalent comment can be made for transitions towards the conduction band when the T_2 state is resonant and the A_1 state is bound. We consider the case $V=-7$ eV in Fig. 7. The peak is very high because of the low threshold value in that case.

3. *Effect of the bound-state symmetry*

The optical perturbation only couples states of different symmetries (because of the $\partial/\partial z$ operator). As we noticed before, an A_1 resonant state is observed in the lower part of the valence band (at -7.3 eV, in the case of the vacancy). The position of this state is shown from Fig. 2(a) not to be very dependent of the potential V. We may then compare the OCS obtained for transitions involving one A_1 or T_2 bound state, both of an energy level of about 0.4 eV in Figs. 8 and 3, respectively. The peak relative to the A_1 resonant state (at about 7.3 eV above the threshold) is observed when the bound state is of T_2 symmetry, not when it is of A_1 symmetry. This shows that the existence and the position of the peaks observed on the OCS spectra are closely linked to the symmetry type of the bound and resonant states. Moreover, as is normal by symmetry, when the bound state is of A_1 symmetry, the light polarization direction is not influent on the OCS curves. On the contrary, when the bound state is of T_2 symmetry, the optical response is modified when the polarization direction is changed (compare Figs. 9 and 3, where transitions occur between t_x and the valence band, when the light is polarized along the [100] and [010] directions, respectively). Finally, we noticed by symmetry that inverting the symmetry axis of the bound state and the light polarization direction does not change the response of the system.

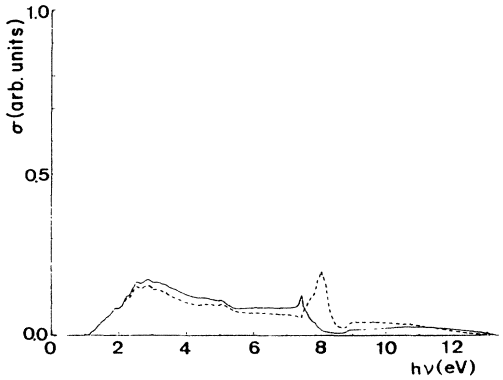

FIG. 5. Same as Fig. 4 for $V=-10$ eV.

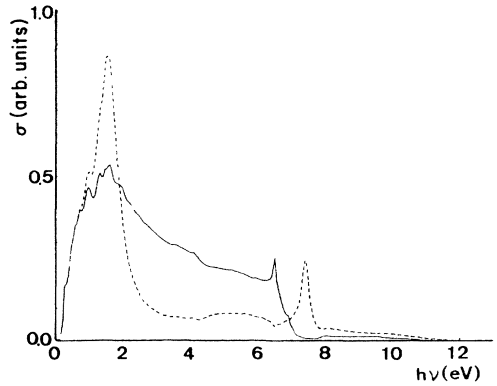

FIG. 6. Same as Fig. 4 for $V=+20$ eV.

IV. DISCUSSION

The substitutional impurities S and Se in silicon give deep levels which are found experimentally[18] at 0.59 eV and 0.52 eV, from the bottom of the conduction-band

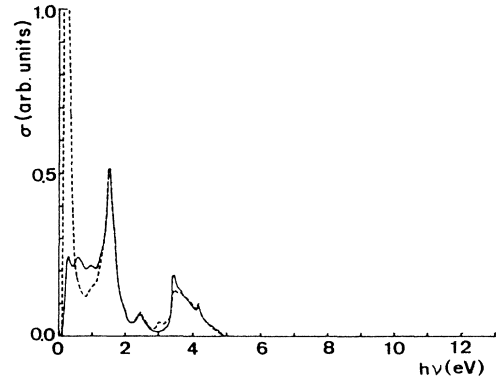

FIG. 7. OCS for transitions between the A_1 bound state associated with $V=-7$ eV and the conduction band (light polarization is indifferent) σ^0: solid line. σ: dashed line.

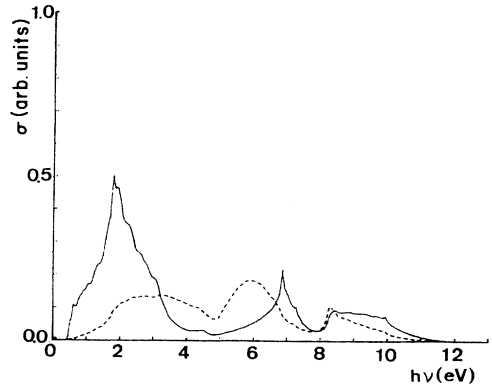

FIG. 8. OCS for transitions between the A_1 bound state associated with $V=-14$ eV and the valence band. σ^0: solid line. σ: dashed line.

edge, respectively. These levels are thought to correspond to the transitions between the charge states + and 2 + .[19] The wave functions associated with these donor levels are thought to be of A_1 symmetry.[8] No maximum is experimentally observed near the threshold for transitions towards the conduction band.[18] The deep level A_1 bound state is well described in our model by the value $V=-14$ eV, which gives the bound-state energy at about 0.42 eV. In that case we also notice a threefold T_2 bound state at 0.85 eV. The associated OCS curve for transitions towards the conduction band is shown in Fig. 10 (by dotted lines) and gives no maximum near threshold, as experimentally observed for Si:S and Si:Se. Experimental transitions from the bound states associated with Si:S and Si:Se to the valence band have shown that the OCS have a linear behavior with photon energy $h\nu$ (Ref. 18) for small energies (at less for $h\nu<0.8$ eV). This particular behavior is also recovered by our calculations in Fig. 8.

A more interesting case is given by Si:Zn. A deep level related to the transition $Zn^- \rightarrow Zn^{2-}$ is experimentally observed at 0.31 eV from the top of the valence band. This state is thought to be of T_2 symmetry.[8] The OCS related to transitions between this level and the valence band shows a maximum for an excitation energy of about 0.6 eV.[20,21] The calculated OCS associated with this level are very close to those obtained in the vacancy case and already reported in Fig. 3. Our calculation shows a maximum of the OCS for approximately $h\nu\simeq 1$ eV, which corresponds to the A_1 resonant state already mentioned

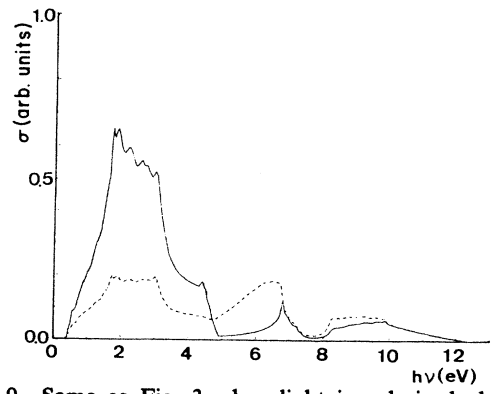

FIG. 9. Same as Fig. 3 when light is polarized along the [010] axis.

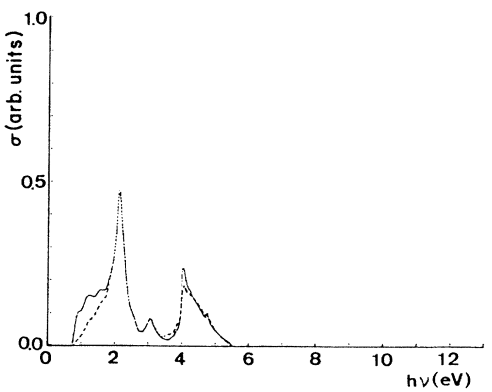

FIG. 10. Same as Fig. 7 for $V=-14$ eV.

above. The difference observed between these values could be explained by the effect of the Coulombic potential region, which is at the heart of the effective-mass approximation and neglected in our model, and which is known to shift the maximum of the OCS towards the threshold value.[2] Let us note that the peak near threshold is recovered only when the band state modifications are taken into account. Indeed when neglecting the effect of the band state modification (see σ^0 on Fig. 3) one recovers, as Jaros *et al.*,[8] that the maximum of the OCS corresponds roughly to the first maximum of the valence band density of states (close to 1.5 eV from the top of the valence band).

V. CONCLUSION

We have demonstrated that the use of unmodified Bloch waves in calculating the OCS can lead to serious errors. We have expressed the OCS in terms of Green's functions localized around the defect center, that is to say, exactly where band state modifications occur. In some cases, the existence of resonant states near band edges can account for the position of maxima of the OCS near thresholds for transitions involving deep levels. However, even in the absence of resonant states, the shape and the amplitude of the OCS are modified. This leads us to conclude that, in practically all cases, it is necessary to take into account the scattering of the Bloch states by the defect potential when calculating the optical cross section.

ACKNOWLEDGMENT

The Laboratoire d'Etude des Surfaces et Interfaces is "Laboratoire d'Etude des Surfaces et Interfaces associé au Centre National de la Recherche Scientifique."

APPENDIX: OCS ASSOCIATED WITH THE VACANCY IN THE MOLECULAR MODEL

We consider a system composed of the four dangling orbitals surrounding the vacancy site. These orbitals are decoupled from the rest of the crystal. If no interaction is set between them, it is well known[16] that a fourfold degenerated state is observed at $\frac{1}{4}(E_s+3E_p)$, where E_s and E_p are the energies of the atomic orbitals of s and p type, respectively. Introducing a coupling $\gamma(\gamma<0)$ between each pair of dangling bonds gives an A_1 state at

$\frac{1}{4}(E_s+3E_p)+3\gamma$ and a T_2 threefold state at $\frac{1}{4}(E_s+3E_p)-\gamma$. These results are in total agreement with those using our more elaborate model developed above. The A_1 state is found to be in the valence band (resonant state) while the T_2 state is in the gap. Optically induced transitions may occur between the T_2 bound state and the valence or conduction band of the crystal. Let us consider, for example, a transition involving the valence band.

The system is defined by four hybrid atomic orbitals as done in Ref. 16. Let us note that $|i,j\rangle$ represent the hybrid orbital located on site i and pointing towards site j. The vacancy is put on central site 0. Then the A_1 resonant state is written:

$$|a_1\rangle=\tfrac{1}{2}(|1,0\rangle+|2,0\rangle+|3,0\rangle+|4,0\rangle)\ . \tag{A1}$$

The bound state is threefold degenerated, a simple and usual basis is given by

$$\begin{aligned}|t_x\rangle&=\tfrac{1}{2}(|1,0\rangle+|2,0\rangle-|3,0\rangle-|4,0\rangle)\ ,\\ |t_y\rangle&=\tfrac{1}{2}(|1,0\rangle-|2,0\rangle+|3,0\rangle-|4,0\rangle)\ ,\\ |t_z\rangle&=\tfrac{1}{2}(|1,0\rangle-|2,0\rangle-|3,0\rangle+|4,0\rangle)\ .\end{aligned} \tag{A2}$$

Only four optical matrix elements are considered between hybrid orbitals pointing towards each other.

Considering a transition between the valence band and the t_x state, we get, for light polarization along the [100] axis:

$$\sigma(h\nu)=-\frac{\beta\hbar^2}{\pi h\nu}\left|\left\langle 1,0\left|\frac{\partial}{\partial x}\right|0,1\right\rangle\right|^2 \times \mathrm{Im}\langle s_0|G_{E_{T_2}-h\nu}|s_0\rangle \tag{A3}$$

where $E_{T_2}=\frac{1}{4}(E_s+3E_p)-\gamma$ and $|s_0\rangle$ is the s-type orbital located on site 0.

Finally, we get

$$\sigma(h\nu)=\frac{\beta\hbar^2}{h\nu}\left|\left\langle 1,0\left|\frac{\partial}{\partial x}\right|0,1\right\rangle\right|^2 n_{s,0}(E_{T_2}-h\nu)\ , \tag{A4}$$

where $n_{s,0}(E)$ is the local (site 0) and partial (s type) density of states at energy E in the valence band.

The effect of the perturbation on band states in the calculation of the OCS is now quite obvious. If we describe bands by unperturbed Bloch states, then the resolvent introduced in Eq. (A3) is G^0 and the density of states in Eq. (A4) is the s-type density of states of the perfect crystal as the translational symmetry is conserved in that case. The OCS $\sigma^0(h\nu)$ is then a function of the s-type density of states.

On the other hand, if we use the exact band functions (that is to say, G instead of G^0), then the density of states appearing in Eq. (A4) is equal to zero at any energy as atom 0 is remote.

Considering transitions involving other bound states or the conduction band obviously leads to the same conclusion. This model clearly shows the influence of local band state perturbation on the OCS calculations. Any refinement of this crude model (such as that developed in our model) must take this effect into account.

[1] G. Lucovsky, Solid State Commun. 3, 299 (1965).
[2] H. B. Bebb, Phys. Rev. **185**, 1116 (1969).
[3] S. Loualiche, A. Nouailhat, G. Guillot, and M. Lannoo, Phys. Rev. B **30**, 5822 (1984).
[4] J. C. Inkson, J. Phys. C **13**, 369 (1981).
[5] M. G. Burt, J. Phys. C **13**, 1825 (1980).
[6] I. L. Jones and J. C. Inkson, Solid State Commun. **51**, 59 (1984).
[7] B. K. Ridley, J. Phys. C **13**, 2015 (1980).
[8] M. Jaros and P. W. Banks, J. Phys. C **15**, 5965 (1982).
[9] J. Bourgoin and M. Lannoo, in *Point Defects in Semiconductors II*, edited by M. Cardona (Springer-Verlag, New York, 1983).
[10] D. L. Dexter in *Solid State Physics*, edited by F. Seitz and D. Turnbull (Academic, New York, 1958), Vol. 6.
[11] J. Bernholc and S. T. Pantelides, Phys. Rev. B **18**, 1780 (1978).
[12] J. Van der Rest and P. Pêcheur, J. Phys. Chem. Solids **45**, 563 (1984).
[13] M. Lannoo and P. Lenglart, J. Phys. Chem. Solids **30**, 2409 (1969).
[14] E. Kauffer, P. Pêcheur, and M. Gerl, J. Phys. C **9**, 2319 (1976).
[15] P. Pêcheur, G. Toussaint, and M. Lanoo, in *Proceedings of the International Conference on Defects and Radiation Effects in Semiconductors, 1980*, IOP Conference Series No. 59, edited by R. R. Hasiguti (IOP, London, 1981), p. 147.
[16] M. Lannoo and J. Bourgoin, in *Point Defects in Semiconductors I*, edited by M. Cardona (Springer-Verlag, New York, 1981).
[17] J. Petit, thesis, Université de Lille I, 1985 (unpublished).
[18] H. G. Grimmeiss and B. Skarstam, Phys. Rev. B **23**, 1947 (1981).
[19] V. A. Singh, U. Lindefelt, and A. Zunger, Phys. Rev. B **27**, 4909 (1983).
[20] Y. I. Zavadskii and B. V. Kornilov, Phys. Status Solidi **42**, 617 (1970).
[21] J. M. Herman and C. T. Sah, J. Appl. Phys. **44**, 1259 (1973).